

MULTIPLE SPOUTS IN A TWO-DIMENSIONAL BED WITH A PERFORATED-PLATE DISTRIBUTOR

CHENG-CHUNG HUANG AND CHIEN-SONG CHYANG*

Department of Chemical Engineering, Chung Yuan Christian University, Chung Li, Taiwan, R.O.C.

Key Words: Multiple Spouts, Perforated Plate, Maximum Spoutable Bed Height

The behavior of multiple spouts above a perforated plate in a 400 mm × 15 mm two-dimensional bed of glass beads with mean diameters from 214 μm to 1095 μm was investigated. The operation of the perforated-plate distributor was taken into account while phase diagrams for the 2-D bed of glass beads were mapped. Two types of incoherent spouting were observed. The stability of multiple spouts was affected by bed height, superficial gas velocity, particle size and distributor design.

Introduction

Since the first proposal of the spouted bed technique by Mathur and Gishler¹²⁾, this technology has been extensively applied. The spouting phenomenon is defined as the formation of a spout immediately above a gas inlet. It consists of three principal regions, i.e. the spout, the annulus and the fountain. Although the major application of this technique is for coarse particles greater than 1 mm or more, Mathur and Gishler¹²⁾ stated that there is a slight overlap between spoutable and fluidizable sizes. Spoutable particles are usually regarded as group D particles in Geldart's⁵⁾ classification of particles. The criteria for spoutability of particles have been suggested to be related to particle size and the density difference between the particles and the gas^{5, 13)} or to be dependent on the gas inlet-to-particle diameter ratio^{1, 6)}.

The behavior of multiple spouts has been investigated in beds with multiple cones¹¹⁾, with a flat base equipped with multiple nozzles⁴⁾, and with a multi-orifice plate¹⁴⁾. Even when the gas flow to each inlet is controlled independently, Epstein and Grace²⁾ have pointed out that spouting stability problems arise when: (a) the pitch between gas inlets is too small, (b) the bed height is increased excessively (but still below the maximum spoutable bed height for a single inlet), and (c) the ratio d_o/d_p is less than 8⁴⁾. The study of spouted beds has been considered to be relevant to the behavior of the grid region in a gas-fluidized bed with a multi-orifice distributor⁹⁾. A comparison of the experimental data and models between a spout and a jet has been made by Filla *et al.*³⁾. However, work concerning both the behavior of multiple spouts and the operation of the multi-orifice distributor is very limited. The jetting phenomenon is defined as the formation of a jet immediately above a gas inlet. The jet is a permanent flame-like cavity above the orifice, and discrete bubbles detach at the end of this cavity.

While the fluidizing gas flows through the orifices of a multi-orifice distributor into a fluidized bed, it may form different gas discharge modes at the orifices, i.e., pulsating jets, bubble plumes or spouts. A spout and a pulsating jet can be regarded as a permanent jet. Grace and Lim⁷⁾ have shown that the criterion given by Chandnani and Epstein¹⁾ for the spoutability of particles, $d_o/d_p \leq 25.4$, can be applied to gas-fluidized bed systems. This criterion has been amply proved for predicting whether permanent jets or bubble plumes are formed in a system. However, it is over-simplified because the effects of several important factors such as jet momentum, particle and gas densities, and bed height are not taken into account. Empirical equations for predicting the transitions of gas discharge modes were presented in a previous work⁸⁾.

The purpose of this work is to investigate the behavior of multiple spouts in a two-dimensional bed equipped with a perforated-plate distributor. An attempt has been made to map phase diagrams concerning both the operation of the distributor and the operation regimes for glass beads with mean diameters ranging from 214 μm to 1095 μm. The interaction between adjacent spouts, the pressure fluctuations corresponding to the regimes observed, and the effect of perforated plate design on the maximum spoutable bed height have been investigated.

1. Experimental

A schematic diagram of the experimental apparatus is shown in Fig. 1. All the experiments were conducted in a two-dimensional fluidized bed, fabricated from acrylic plates. The cross-section of the bed was 400 mm × 15 mm. Iron plates, on which an array of 3 or 7 orifices were drilled, were used as distributors. The orifice diameters were from 1.5 mm to 5 mm. The plenum was 0.45 m in height. Glass beads with mean diameters from

* Received January 12, 1993. Correspondence concerning this article should be addressed to C.-S. Chyang.

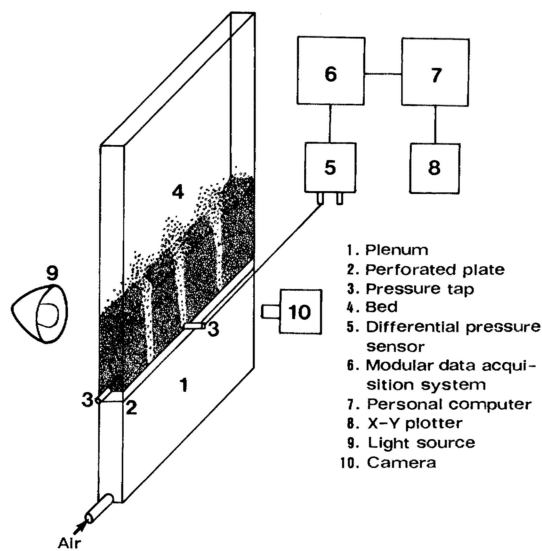


Fig. 1 Schematic diagram of the experimental apparatus

Table 1. Experimental Conditions

| | |
|-------------------------------------|----------------------------------|
| Bed Cross Section (mm × mm) | 400 × 15 |
| Particles | Glass Beads |
| Mean Diameter (μm) | 214, 359, 545, 650, 1095 |
| Minimum Fluidization Velocity (m/s) | 0.048, 0.074, 0.186, 0.283, 0.55 |
| Distributor | Perforated Plate |
| Orifice Number | 3, 7 |
| Orifice Pitch (mm) | 100, 50 |
| Orifice Diameter (mm) | 1.5, 2.26, 3, 4.1, 5 |

214 μm to 1095 μm were used as the bed materials. A camera was used to photograph the bed during operation. All the experimental conditions are shown in Table 1.

On the sidewall and at the centerline of the front wall, pressure taps were installed 5 mm from the perforated plate for measuring pressure fluctuations. The inside opening of the pressure tap was covered with a 200-mesh screen to prevent solids from entering the tap. The signals measured from the pressure tap on the front wall were regarded as those measured at the orifice, because the tap corresponded to the orifice located in the middle of the plate.

The pressure fluctuations were measured by connecting the pressure tap to a SenSym SCX01DNC differential-pressure sensor having two input channels. The low-pressure input was exposed to the atmosphere. The operating pressure of the differential-pressure sensor was 0 to 6.9 kPa. Its accuracy was $\pm 0.2\%$ of the full-scale span output. The output signal of the differential-pressure sensor was transmitted to an ACUREX 7000-MDAS modular data acquisition system. The 7000-MDAS was used to acquire pressure fluctuation signals as well as the fast Fourier transform of the time domain data in order to obtain frequency domain data. A personal computer was used to control the 7000-MDAS for implementing the sampling and for spectral analysis of pressure fluctuation signals. The sampling interval of the pressure fluctuations was 25 ms. For each test 5120



(a)



(b)



(c)

Fig. 2 Multiple spouts above the perforated plate at various fluidization numbers. $d_p = 650 \mu\text{m}$, $H = 92 \text{ mm}$, $N = 7$, $d_o = 2.26 \text{ mm}$, UIU_{mf} : (a) 1.87 (b) 2.78 (c) 3.31.

points were collected and processed. The total sampling time was 128 seconds.

The maximum spoutable bed height, H_m , was determined by the following procedure. At a certain bed height the superficial gas velocity was increased. If a spout formed at each orifice, the bed height might be either lower than H_m or equal to H_m . The bed height was then increased. The bed height must be higher than H_m if spouts could not be formed at any superficial gas velocity. The bed height was reduced gradually till a steady spout obviously formed at each orifice. At this point, the bed height was taken as the maximum spoutable bed height.

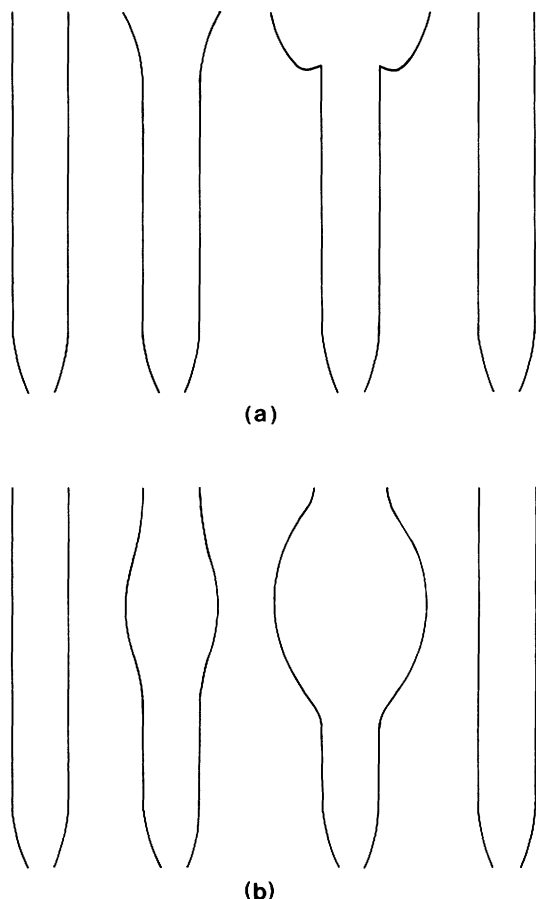


Fig. 3 Variation of spout shape for (a) type I I.S. and (b) type II I.S.

2. Results and Discussion

2.1 Interaction between adjacent spouts

The photographs in **Fig. 2** show the multiple spouts for 650- μm glass beads above a perforated plate, which has seven orifices, at various superficial gas velocities. The objects appearing in the middle of each photograph are an array of pressure taps installed on the front wall of the two-dimensional bed. At a low fluidization number, 1.87, vertical spouts above most of the orifices are illustrated in photograph (a). Distortion of the spout shape occurred near the side wall because of the hindering of the flow of particles, which caused a nonuniform particles flow between the two sides of the spout. In the regions between spouts, particles flowed downward and radially toward the spout. With the fluidization number increased to 2.78, photograph (b) shows the distortion of the spouts. The adjacent spouts on the right side appeared to interact with each other. The fountains of the interacting spouts could not be well defined. The particles flow between the interacting spouts became random. Photograph (c) shows a very significant interaction between spouts at a fluidization number of 3.31. The particles flow pattern no longer resembled that in a conventional spouted bed. The interaction of spouts shown in **Fig. 2** at various superficial gas velocities considerably resembles the interaction process described by Wu and

Whiting¹⁶⁾ for two jets in a semicircular bed.

When the interaction between spouts occurred at high gas velocities it was found that the dead zones between orifices tended to diminish. This resulted from two causes: (1) particles stirred by the interacting spouts and (2) particles fluidized by air leaked from the spout. Wen *et al.*¹⁵⁾ proposed a mechanism for the transition of the gas discharge mode from jetting to bubbling at orifices. They claimed that, as the gas velocity was increased, jetting would transit to bubbling if the dead zones between orifices were eliminated. However, that process was not observed throughout this work.

It was noted that interacting spouting did not occur at a bed height less than H_m . At a lower bed height, the fountain height increased while the gas velocity was increased. As the gas velocity was further increased, dancing spouts were observed. The spouts and fountains would shake left and right.

2.2 Incoherent spout

In a conventional spouted bed, incoherent spouting (I.S.) has been observed^{1, 11)}. In this work, two types of incoherent spouting were observed, as shown in **Fig. 3**. When type I I.S. occurred, the variation of spout shape is as shown in **Fig. 3** (a). For large particles, type I I.S. was observed when waves appeared along the spout-annulus interface near the bed surface, which caused the fountain to collapse. The waves would grow, and eventually this led to a pinch point where a non-fully developed bubble formed and erupted on the bed surface. The process was quite similar to that described by Chandnani and Epstein¹⁾. If the bed height was increased when an incoherent spouting occurred, the operation regime would transit to jetting. For fine particles, jets followed by bubble plumes usually appeared first as the superficial gas velocity was increased. Then the jet penetration length increased and the bubbles in the bubble plume tended to coalesce in the axial direction as the superficial gas velocity was increased. Type I I.S. occurred when the pinch point reached a height where a non-fully developed bubble formed and erupted through the bed surface.

As to type II I.S., the variation of spout shape is shown in **Fig. 3** (b). It occurred when waves appeared along the spout-annulus interface near the middle of the spout. This causes a fluctuation phenomenon characterized by expanding and shrinking of the spout-annulus interface. The flow of particles in the regions between spouts was disturbed during the variation in spout shape. The type II I.S. was usually found in multiple-spouted beds of 214- μm and 359- μm glass beads.

2.3 Phase diagrams

Figure 4 shows experimental phase diagrams for 214- μm to 1095- μm glass beads in a multiple-spouted bed when a perforated plate with three 3-mm orifices was used as the distributor. To avoid the hysteresis effect, the superficial gas velocity was quickly increased to make all the orifices operative. The data shown in the phase diagrams were obtained by further increasing or

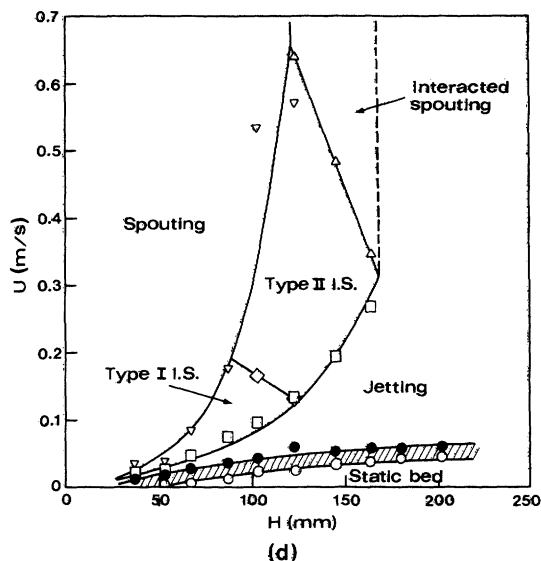
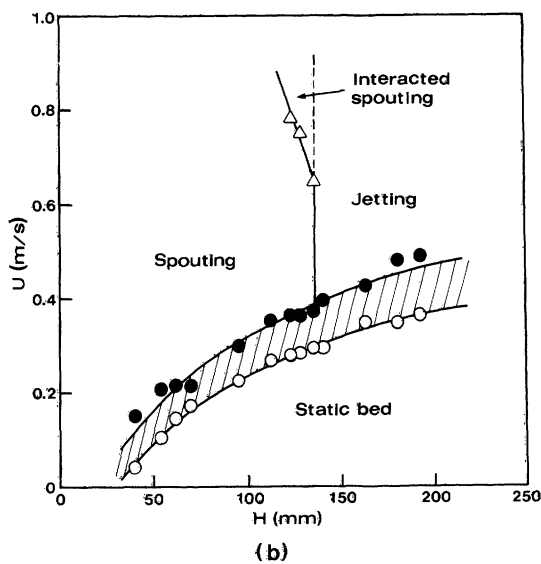
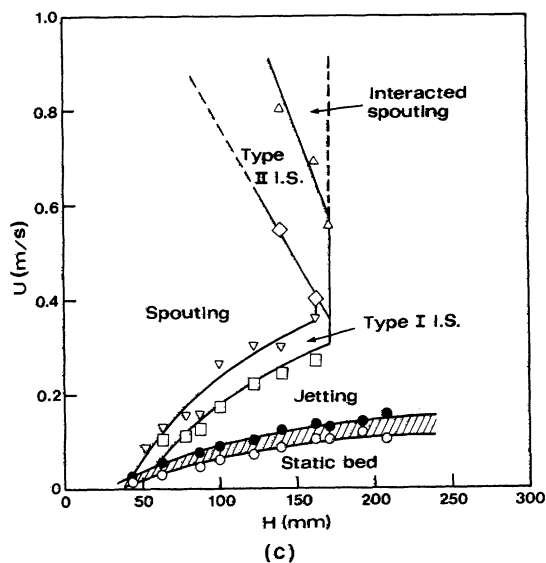
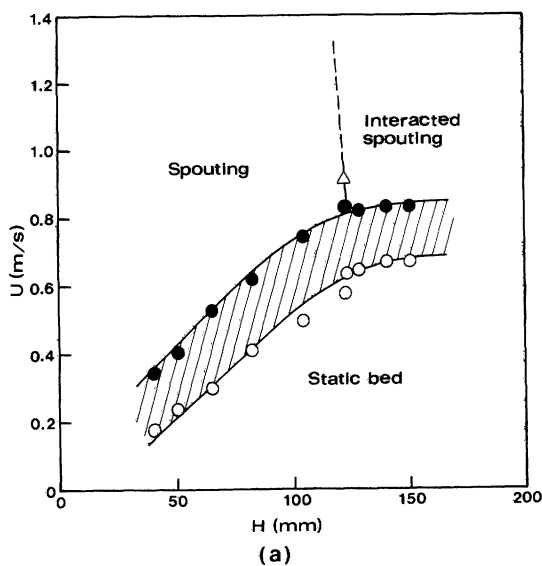


Fig. 4 Phase diagram for glass beads in the multiple-spouted bed. $N = 3$, $d_o = 3$ mm. (a) $d_p = 1095 \mu\text{m}$ (b) $d_p = 650 \mu\text{m}$ (c) $d_p = 359 \mu\text{m}$ (d) $d_p = 214 \mu\text{m}$

decreasing the superficial gas velocity. The operation of the perforated plate was taken into account in these phase diagrams and is represented by the regions with slanted lines.

For a given bed height, the lower limit (marked with blank circle) represents the point at which only one orifice became operative. The upper limit (marked with black circle) represents the point at which all the orifices were operative. Various symbols shown in the phase diagrams are used to represent the experimental data points at the boundary between different phase regions. The dashed line shown in the phase diagram is used to project the boundary of different phase regions. The precise boundary cannot be illustrated for lack of exact data.

By visual observation, an orifice was regarded to be operative when a spout formed or when bubbles detached from the end of a jet could flow up to the bed surface. An orifice, at which a permanent high void stood which neither penetrated the bed surface nor broke into a bubble, was considered to be nonoperative. The upper limit of the region with slanted lines shown in the phase

diagram, in fact, represents the relationship between the minimum superficial gas velocity, which made all the orifices operative, and the bed height in the system tested. Unlike a conventional spouted bed or a multiple-spouted bed with independent controlled air flow to each inlet, the problem concerning even distribution of gas flow through the orifices of a distributor is very important in a gas-fluidized bed. Therefore, in addition to the interaction of adjacent spouts, spouting stability is also affected by the nonoperative orifices.

For a bed of 1095- μm glass beads, Fig. 4 (a) shows the regimes with a static bed, spouting and interacting spouting. For a bed of 650- μm glass beads, Fig. 4 (b) shows the regimes with a static bed, spouting, interacting spouting and jetting. The term "Jetting", instead of "Bubbling", is used to represent the regime in which jet bubbles formed in the bed. In a fluidized bed equipped with a multiorifice distributor, the term "Bub-

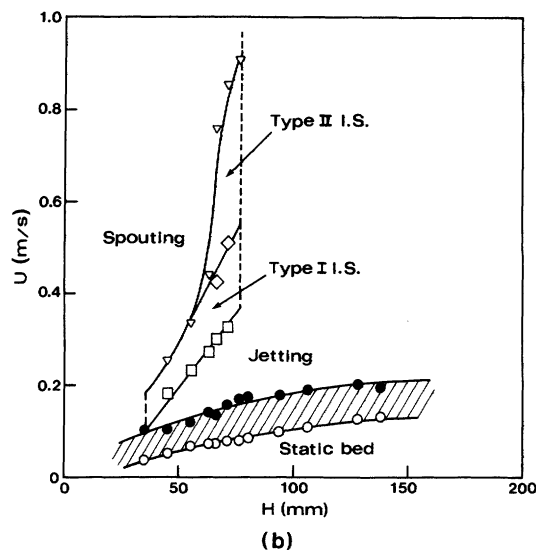
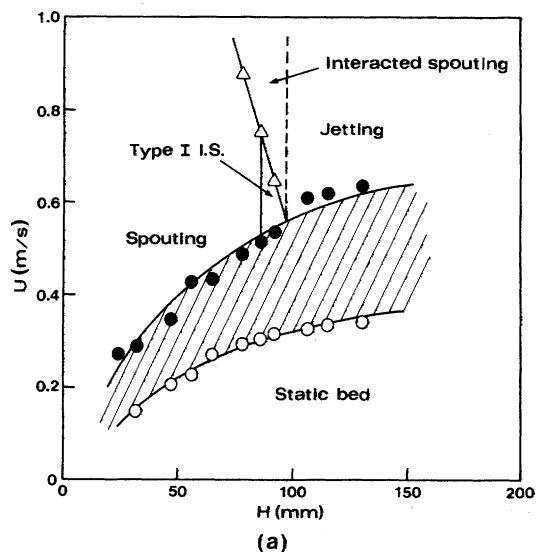


Fig. 5 Phase diagram for glass beads in the multiple-spouted bed. $N = 7$, $d_o = 3$ mm. (a) $d_p = 650 \mu\text{m}$ (b) $d_p = 359 \mu\text{m}$

bling” can be used for the gas discharge mode when bubbles form immediately at the orifices; therefore, ambiguity can be avoided if “Jetting” and “Bubbling” are used respectively to characterize the different gas discharge modes in the phase diagrams. Both type I and type II I.S. appear in Figs. 4 (c) and 4 (d) for 359- μm and 214- μm glass beads. Jetting was found to be followed by incoherent spouting and then by stable spouting as the superficial gas velocity was increased. This clearly implies that, for a bed of fine particles, spouting results from the increase of jet penetration and the coalescence of bubbles in the bubble plume at the end of the jets.

In comparison with Fig. 4, Fig. 5 shows the phase diagrams for 650- μm and 359- μm glass beads, when a perforated plate with seven 3-mm orifices was used. It reveals that the difference between the superficial gas velocity which made only one orifice operative and that which made all the orifices operative was larger when a perforated plate with a higher open area ratio was used. Generally speaking, the instability of multiple spouts

Table 2. Relationships of U_{mf} and U_{ms} , U_M and U_I at H_m

| N (-) | d_o (mm) | d_p (μm) | H_m (mm) | $(U_{ms})_{H_m}/U_{mf}$ | $(U_M)_{H_m}/U_{mf}$ | $(U_I)_{H_m}/U_{mf}$ | | |
|------------|---------------|----------------------------|---------------|-------------------------|----------------------|----------------------|------|---|
| 3 | 3 | 1095 | 123 | 1.49 | 1.49 | 1.15 | | |
| | | 650 | 135 | 1.37 | 1.37 | 1.06 | | |
| | | 545 | 141 | 2.5 | 1.44 | 1.07 | | |
| | | 359 | 162 | 4.83 | 1.74 | 1.31 | | |
| 3 | 4.1 | 214 | 123 | 11.92 | 0.97 | 0.58 | | |
| | | 1095 | 124 | 1.46 | 1.46 | 1.07 | | |
| | | 650 | 139 | 1.66 | 1.18 | 1.0 | | |
| | | 545 | 160 | 2.61 | 1.4 | 1.11 | | |
| 3 | 4.1 | 359 | 157 | 6.54 | 1.68 | 1.28 | | |
| | | 214 | 109 | 11.0 | 0.98 | 0.54 | | |
| | | 7 | 1.5 | 1095 | - | - | - | - |
| | | 650 | | 77 | 1.81 | 1.81 | 0.98 | |
| 545 | 90 | 2.03 | | 1.89 | 1.05 | | | |
| 359 | 80 | 3.15 | | 1.61 | 1.07 | | | |
| 7 | 4.1 | 214 | 69 | 1.98 | 0.77 | 0.4 | | |
| | | 1095 | 72 | 1.64 | 1.64 | 1.25 | | |
| | | 650 | 79 | 2.19 | 1.53 | 1.0 | | |
| | | 545 | 81 | 3.89 | 1.48 | 1.13 | | |
| 7 | 4.1 | 359 | 70 | 8.36 | 2.0 | 1.11 | | |
| | | 214 | 61 | 7.35 | 1.48 | 0.58 | | |

increased when a distributor with a smaller pitch was used. It is evident that type I I.S. appears in Fig. 5 (a) for 650- μm glass beads. According to the results mentioned above, the stability of multiple spouts was affected by bed height, superficial gas velocity, particle size, interaction between adjacent spouts, and operativeness of the orifices. The last two factors are especially governed by the multi-orifice distributor design.

The controversy about the relationship of $(U_{ms})_{H_m}$ and U_{mf} has been discussed by Littman and Morgan¹⁰. They claimed that $(U_{ms})_{H_m}$ should be approximately equal to U_{mf} . Table 2 shows the relationships of the minimum fluidization velocity and the minimum spouting velocity, the minimum velocity which makes all the orifices operative and the gas velocity which makes only one orifice operative at H_m . It is seen that the ratios of $(U_{ms})_{H_m}/U_{mf}$ are larger than unity, and that very high values were obtained for fine particles. This resulted from the fact that there is a connection of $(U_{ms})_{H_m}$ and U_{mf} based on the measurement of H_m ¹⁰. In this work, H_m was taken at maximum bed height when a stable spout could be formed at each orifice. When the superficial gas velocity was not high enough, spouts formed at some of the orifices, while jetting or a static bed was observed at other orifices. The superficial gas velocity had to be increased so that a stable spout could form at each orifice. Thus, the minimum spouting velocity for a multiple-spouted bed equipped with a multi-orifice distributor must be higher than that for a single spout. Except for 214 μm glass beads, Table 2 shows that $(U_I)_{H_m}/U_{mf}$ values are in the range from 1 to 1.3. When there was only one operative orifice, a stable spout was usually observed for 359- μm to 1095- μm glass beads. This implies that the minimum spouting velocity for a single spout in a multiple-spouted bed is also close to U_{mf} . For 214- μm glass beads, the maldistribution of gas

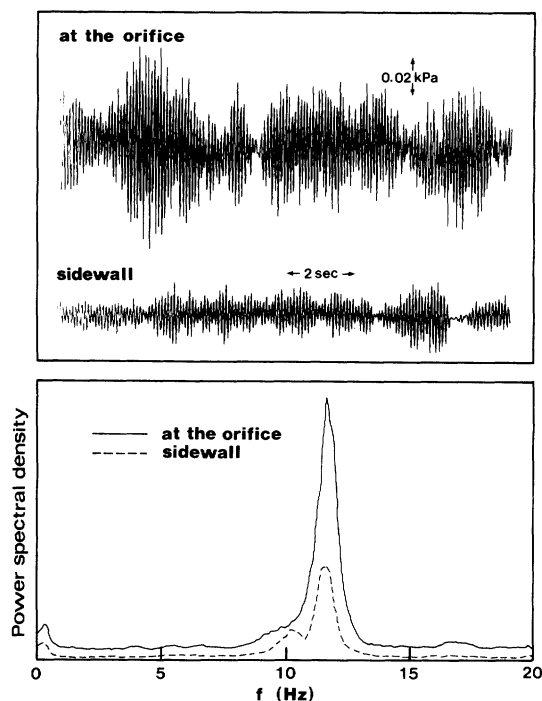


Fig. 6 Pressure fluctuations and corresponding power spectral densities for stable spouting. $d_p = 545 \mu\text{m}$, $H = 80 \text{ mm}$, $U/U_{mf} = 2.58$, $N = 3$, $d_o = 3 \text{ mm}$.

flow through the distributor was more serious. Channeling also occurred easily. At a superficial gas velocity much lower than U_{mf} the gas tended to flow through one orifice and make it operative. It is thus reasonable that $(U_1)_{H_m}/U_{mf}$ is less than unity for $214\text{-}\mu\text{m}$ glass beads. Table 2 also shows that $(U_M)_{H_m}/U_{mf}$ is in the range from about 1 to 2.

2.4 Pressure fluctuations

Figure 6 shows the pressure fluctuations and the corresponding power spectral densities as typical stable spouting occurred in the two-dimensional bed. Generally speaking, the power spectral densities show a narrow distribution with a sharp peak which corresponds to a high major frequency for stable spouting. No significant minor frequencies were found. In this case, the major frequencies measured from the taps on the side wall and at the orifice appear at 11.6 Hz. The signals measured at the orifice were found to be more significant than those measured from the tap on the side wall. The characteristics of the pressure fluctuations shown in **Fig. 6** for stable spouting in the multiple-spouted bed are similar to those reported in the previous work⁸⁾ obtained in a two-dimensional bed equipped with a single nozzle.

As the spouting began to dance, **Fig. 7** shows that the pressure fluctuations compose a periodic main wave. This was especially obvious for the signals measured from the tap on the side wall. This resulted from the fact that the spouts and the fountains shook left and right slowly or quickly, depending on the superficial gas velocity. In this case, the major frequencies were found to appear at about 0.4 Hz. As interacting spouting occurred, the pressure fluctuations that occurred are

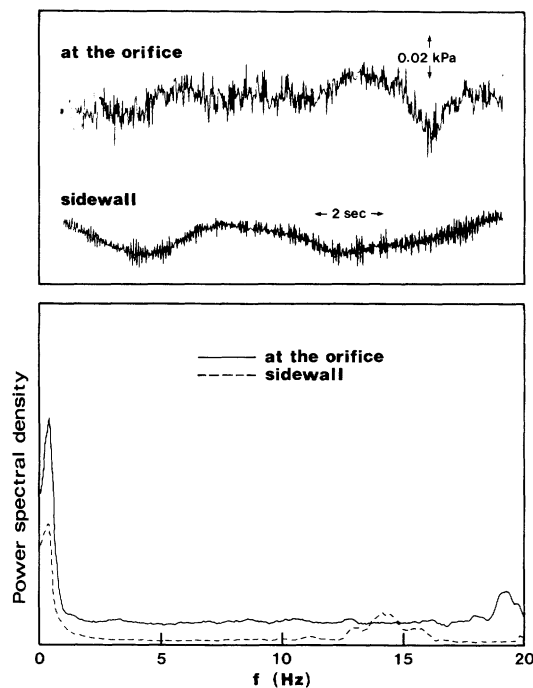


Fig. 7 Pressure fluctuations and corresponding power spectral densities for dancing spouts. $d_p = 650 \mu\text{m}$, $H = 80 \text{ mm}$, $U/U_{mf} = 1.23$, $N = 3$, $d_o = 3 \text{ mm}$.

shown in **Fig. 8**. In this case, stable spouting occurred at the orifice near the pressure tap on the side wall. The spouts at the other two orifices interacted with each other. A periodic main wave composed by the fluctuation signals was also found. The power spectral density distributions measured from the side wall and at the orifice were found to have a similar trend. The major frequencies still appear at 0.4 Hz. Minor frequencies are observed at about 6 Hz.

2.5 Maximum spoutable bed height

The effect of orifice pitch to orifice diameter ratio, P/d_o , on the maximum spoutable bed height to orifice diameter ratio, H_m/d_o , is shown in **Fig. 9** with mean particle diameter as the parameter. This figure, in which log-log coordinates are used, reveals that H_m/d_o increases linearly as P/d_o increases. Different slopes of the linear relationships for group B and group D particles were found. Solid lines and dashed lines are used in **Fig. 9** to represent the discrepancy. This implies that H_m/d_o is a power function of P/d_o . The powers, which are the slopes of the lines in **Fig. 9**, are 1.12 and 0.72 for groups B and D glass beads respectively. According to Geldart's classification, $650\text{-}\mu\text{m}$ glass beads are usually regarded to be at the margin between groups B and D; however, they were regarded as group D particles in this work, because it was found that $650\text{-}\mu\text{m}$ and $1095\text{-}\mu\text{m}$ glass beads had the same power for the relationship between H_m/d_o and P/d_o .

At a given P/d_o , **Fig. 9** also shows that H_m/d_o increases as particle diameter increases for group B particles. On the contrary, H_m/d_o decreases as particle diameter increases for group D particles. The results

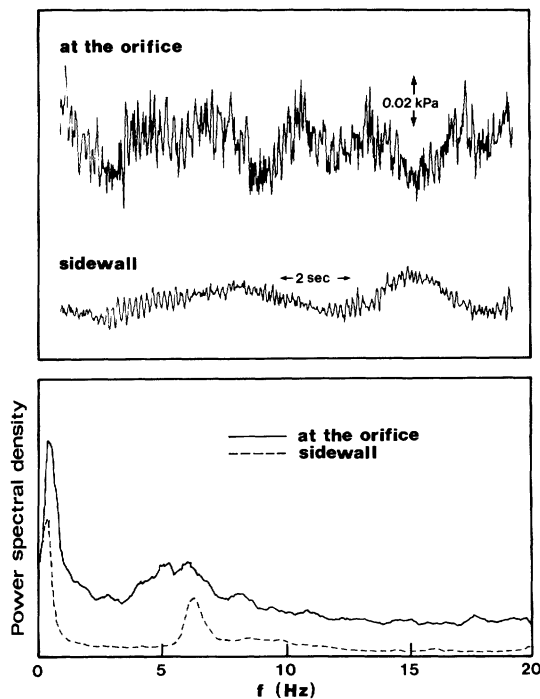


Fig. 8 Pressure fluctuations and corresponding power spectral densities for interacting spouting. $d_p = 545 \mu\text{m}$, $H = 80 \text{ mm}$, $U/U_{mf} = 4.15$, $N = 3$, $d_o = 3 \text{ mm}$.

shown in Fig. 9 may not be suitably applied under conditions out of the range tested in this work, especially when P/d_o is less than 10. The interactions between spouts significantly reduce the maximum spoutable bed height, while P/d_o is too small.

Conclusions

In this work, the behavior of multiple spouts was investigated in a $400 \text{ mm} \times 15 \text{ mm}$ two-dimensional bed equipped with a perforated plate. Glass beads with mean diameters from $214 \mu\text{m}$ to $1095 \mu\text{m}$ were used as the particles. Two types of incoherent spout were observed in this work. Both the operation of the perforated plate and the operation regimes for the glass beads were taken into account while a phase diagram was mapped. The stability of multiple spouts was affected by bed height, superficial gas velocity, particle size, interaction between adjacent spouts, and operativeness of the orifices. The last two factors are, actually, governed due to the distributor design.

The power spectral density distributions of the pressure fluctuations measured at the orifice and from the side wall for the regimes observed in this work revealed the same major frequency. As stable spouting occurred, a narrow distribution of the power spectral density with a sharp peak corresponding to a very high major frequency was observed.

H_m/d_o was found to be a power function of P/d_o . The powers were 1.12 and 0.72 for groups B and D glass beads respectively. At a given P/d_o , H_m/d_o increased as particle diameter increased for group B glass beads. As

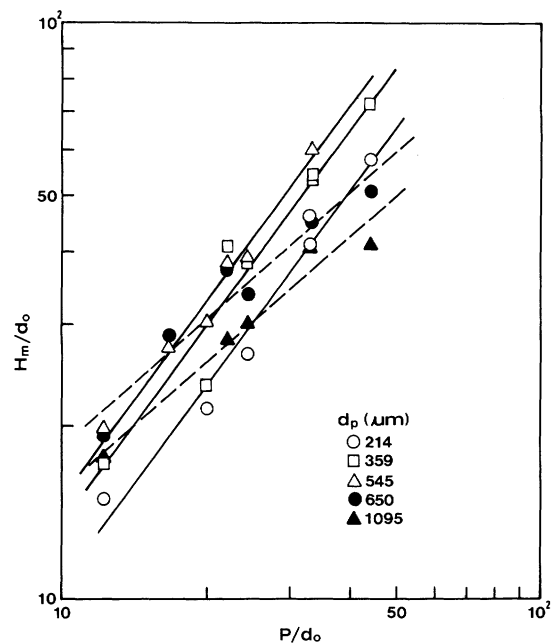


Fig. 9 Effect of orifice pitch to orifice diameter ratio on maximum spoutable bed height to orifice diameter ratio

to group D glass beads, H_m/d_o decreased as particle diameter increased.

Acknowledgements

The authors are grateful to the National Science Council, R.O.C., for support to this work under grant NSC 79-0402-E033-02.

Nomenclature

| | | |
|----------|--|-------|
| d_o | = orifice diameter | [m] |
| d_p | = particle diameter | [m] |
| f | = frequency of pressure fluctuations | [Hz] |
| H | = bed height | [m] |
| H_m | = maximum spoutable bed height | [m] |
| N | = orifice number | [-] |
| U | = superficial gas velocity | [m/s] |
| U_M | = minimum superficial gas velocity at which all orifices are operative | [m/s] |
| U_{mf} | = minimum fluidization velocity | [m/s] |
| U_{ms} | = minimum spouting velocity | [m/s] |
| U_1 | = superficial gas velocity at which only one orifice becomes operative | [m/s] |
| P | = orifice pitch | [m] |

Literature Cited

- 1) Chandnani, P.P. and N. Epstein, in *Fluidization V*, K. Ostergaard and A. Sorensen, Eds., Engineering Foundation, New York, pp. 233 (1986)
- 2) Epstein, N. and J.R. Grace, in "Handbook of Powder Science and Technology", M.E. Fayed and L. Otten, Eds., Van Nostrand Reinhold, New York (1984)
- 3) Filla, M., L. Massimilla and S. Vaccaro: *Can. J. Chem. Eng.*, **61**, 370 (1983)
- 4) Foong, S.K., R.K. Barton and J.S. Ratcliffe, *Mech. and Chem. Eng. Trans. Instn. Engrs., Aust.*, MCII (1, 2), 7-12 (1975)
- 5) Geldart, D.: *Powder Technol.*, **7**, 285 (1973)
- 6) Ghosh, B.: *Indian Chem. Engr.*, **7**, 16 (1965)
- 7) Grace, J.R. and C.J. Lim: *Can. J. Chem. Eng.*, **65**, 160 (1987)
- 8) Huang, C.C. and C.S. Chyang: *J. Chem. Eng. Japan*, **24**, 633 (1991)
- 9) Lefroy, G.A. and J.F. Davidson: *Trans. Instn. Chem. Engrs.*, **47**, 120 (1969)
- 10) Littman, H. and M.H. Morgan, III: *Can. J. Chem. Eng.*, **61**, 269

- (1983)
- 11) Mathur, K.B. and N. Epstein, *Spouted Beds*, Academic Press, New York (1974)
 - 12) Mathur, K.B. and P.E. Gishler: *AIChE J.*, **1**, 157 (1955)
 - 13) Molerus, O., *Powder Technol.*, **33**, 81 (1982)
 - 14) Rooney, N.M. and D. Harrison: *Powder Technol.*, **9**, 227 (1974)
 - 15) Wen, C.Y., N.R. Deole and L.H. Chen: *Powder Technol.*, **31**, 175 (1982)
 - 16) Wu, C.S. and W.B. Whiting: *Chem. Eng. Commun.*, **73**, 1 (1988)